

Optical Engineering

OpticalEngineering.SPIEDigitalLibrary.org

Combined tunable diode laser absorption spectroscopy and monochromatic radiation thermometry in ammonium dinitramide-based thruster

Hui Zeng
Dongbin Ou
Lianzhong Chen
Fei Li
Xilong Yu

SPIE.

Hui Zeng, Dongbin Ou, Lianzhong Chen, Fei Li, Xilong Yu, "Combined tunable diode laser absorption spectroscopy and monochromatic radiation thermometry in ammonium dinitramide-based thruster," *Opt. Eng.* **57**(2), 026106 (2018), doi: 10.1117/1.OE.57.2.026106.

Combined tunable diode laser absorption spectroscopy and monochromatic radiation thermometry in ammonium dinitramide-based thruster

Hui Zeng,^a Dongbin Ou,^a Lianzhong Chen,^a Fei Li,^b and Xilong Yu^{b,c,*}

^aChina Academy of Aerospace Aerodynamics, Beijing Key Laboratory of Arc Plasma Application Equipment, Beijing, China

^bChinese Academy of Sciences, Institute of Mechanics, Key Laboratory of High Temperature Gas Dynamics, Beijing, China

^cUniversity of Chinese Academy of Sciences, School of Engineering Science, Beijing, China

Abstract. Nonintrusive temperature measurements for a real ammonium dinitramide (ADN)-based thruster by using tunable diode laser absorption spectroscopy and monochromatic radiation thermometry are proposed. The ADN-based thruster represents a promising future space propulsion employing green, nontoxic propellant. Temperature measurements in the chamber enable quantitative thermal analysis for the thruster, providing access to evaluate thermal properties of the thruster and optimize thruster design. A laser-based sensor measures temperature of combustion gas in the chamber, while a monochromatic thermometry system based on thermal radiation is utilized to monitor inner wall temperature in the chamber. Additional temperature measurements of the outer wall temperature are conducted on the injector, catalyst bed, and combustion chamber of the thruster by using thermocouple, respectively. An experimental ADN thruster is redesigned with optimizing catalyst bed length of 14 mm and steady-state firing tests are conducted under various feed pressures over the range from 5 to 12 bar at a typical ignition temperature of 200°C. A threshold of feed pressure higher than 8 bar is required for the thruster's normal operation and upstream movement of the heat release zone is revealed in the combustion chamber out of temperature evolution in the chamber. © 2018 Society of Photo-Optical Instrumentation Engineers (SPIE) [DOI: [10.1117/1.OE.57.2.026106](https://doi.org/10.1117/1.OE.57.2.026106)]

Keywords: tunable diode laser absorption spectroscopy; monochromatic radiation thermometry; ammonium dinitramide-based thruster.

Paper 171802 received Nov. 11, 2017; accepted for publication Jan. 16, 2018; published online Feb. 9, 2018.

1 Introduction

Over the last decade, interests for green space propulsion have gained additional attention and a new green liquid monopropellant has been developed based on ammonium dinitramide (ADN). ADN monopropellant is a liquid blend of ADN $[\text{NH}_4\text{N}(\text{NO}_2)_2]$, water, and methanol.¹ In this mixture, ADN is regarded as a high energetic oxidizer, dissolving in water fueled by methanol. Owing to low toxicity, safer handling, and high performance of the monopropellant, the ADN-based thruster stands to be a logical replacement for hydrazine-based systems in small satellite missions, and applications of ADN liquid monopropellant for spacecraft propulsion have been discussed in Ref. 2. Currently, the ADN-based thruster has been developed and successful in-space demonstration of the high performance green propulsion (HPGP) system based on a 1 N thruster has been implemented on the PRISMA spacecraft platform.^{3–6} It is of great significance to obtain quantitative understandings of the thruster performance, for lack of experimental study for this new thruster. As temperature is the fundamental thermodynamic properties, experimental temperature measurements of combustion gas, inner wall in the thruster chamber, and outer wall of the thruster allow for analyzing the thermal evolution of the thruster when operation.

Techniques for temperature measurement are extensive, utilizing the characteristics, such as thermoelectricity, temperature-dependent variation of the resistance of electrical

conductors, fluorescence, and spectra.⁷ Traditional methods are to directly contact with the medium, which is disadvantageous and inapplicable for detection of flow parameters for a small-sized ADN-based thruster. Two nonintrusive methods are utilized to infer temperature of combustion gas and inner-wall in the chamber, respectively. One method is laser absorption spectroscopy (LAS) to infer gas temperature in the center portion of the thruster chamber. The laser-based sensors have various applications capable of giving nonintrusive, *in situ* detection for real, harsh combustion environments.⁸ Temperature measurements of combustion gas are presented in various facilities, such as Hencken burner, shock tube, and direct-connect model scramjet combustors.^{9–12} Another method is monochromatic radiation thermometry to infer temperature of the inner-wall in the chamber, in which this technique is useful to measure temperatures over the range of 50 to 6000 K based on thermal radiation.⁷ Monochromatic radiation thermometry is a mature technique to monitor temperature, and applications have been made to measure temperatures of flame and metal materials based on gray body assumption.^{13,14} Advances in characterizing three-dimensional temperature distribution of the combustion chamber are achieved by using two-color radiation thermometry.^{15,16}

This paper combines a laser-based sensor and monochromatic radiation thermometry to give *in-situ* measurements of temperature under high temperature (up to 1500 K) conditions in a real ADN-based thruster. Scanned-wavelength

*Address all correspondence to: Xilong Yu, E-mail: xlyu@imech.ac.cn

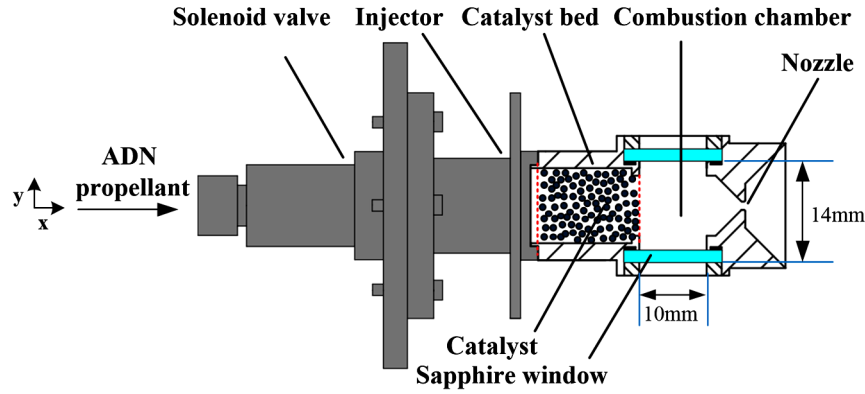


Fig. 1 Schematic of the ADN-based thruster.

direct absorption spectroscopy is utilized and temperatures of combustion gas are attained from the ratio of two H_2O transitions with thermometry range of 500 to 2000 K, while a single monochromatic CCD camera is utilized to obtain the relationship between pixel grayscale and temperature, and then temperatures of the inner-wall in the chamber are derived from calibration data based on Wien's law.

2 Method

2.1 Laser Absorption Spectroscopy

A brief discussion of LAS is presented in this paper since the theory is readily available in previous work.^{9,17} Direct absorption spectroscopy for a monochromatic radiation at frequency ν is governed by the Beer-Lambert's law, which relates the transmitted intensity I_v through a uniform gas medium of length L (cm) to the incident intensity I_0 as follows:

$$\frac{I_v}{I_0} = \exp[-PX_{\text{abs}}S(T)\phi(\nu - \nu_0)L], \quad (1)$$

where P (bar) is the pressure of gas medium, X_{abs} is the mole fraction of the absorbing species, $S(T)$ ($\text{cm}^{-2}\text{atm}^{-1}$) is the line strength of the transition at temperature T (K), L is the pathlength, and $\phi(\nu - \nu_0)$ is the lineshape function at wavelength center of ν_0 . The lineshape function $\phi(\nu - \nu_0)$ is normalized such that $\int_{-\infty}^{+\infty} \phi(\nu - \nu_0) d\nu = 1$ and the integrated absorbance (cm^{-1}) can be expressed as follows:

$$A = PX_{\text{abs}}S(T)L. \quad (2)$$

Gas temperature is obtained from the ratio of the two-line integrated absorbance area:

$$T = \frac{\frac{hc}{k}(E_2'' - E_1'')}{\ln \frac{A_1}{A_2} + \ln \frac{S_2(T_0)}{S_1(T_0)} + \frac{hc}{k} \frac{(E_2'' - E_1'')}{T_0}}, \quad (3)$$

where h (Js) is Planck's constant, c (cm/s) is the speed of light, k (J/K) is Boltzmann's constant, E_i'' (cm^{-1}) ($i = 1, 2$) is the lower state energy of the transition, T_0 (K) is the reference temperature of 296 K, and $S(T_0)$ ($\text{cm}^{-2}\text{atm}^{-1}$) is the line strength of the transition at temperature T_0 (K).

2.2 Monochromatic Radiation Thermometry

The radiation intensity at a given wavelength is governed by Planck's distribution:

$$I(\lambda, T) = \frac{\varepsilon(\lambda)}{\pi} \frac{C_1}{\lambda^5} \frac{1}{\exp(C_2/\lambda T) - 1}, \quad (4)$$

where I is the monochromatic radiation intensity at a given wavelength λ and a given temperature T , $\varepsilon(\lambda)$ is the monochromatic emissivity for a given wavelength λ , $C_1 = 2hc^2$, $C_2 = hc/k$, h is the Planck constant, c is the speed of light, and k is the Boltzmann constant. The formula could be simplified using Wien's law of radiation for a temperature range from 800 to 2000 K and wavelength over the range of 300 to 1000 nm:¹⁸

$$I(\lambda, T) = \frac{\varepsilon(\lambda)}{\pi} \frac{C_1}{\lambda^5} \exp(-C_2/\lambda T). \quad (5)$$

Based on the assumption of a constant emissivity ε for gray body, the relationship between the radiation intensity I at wavelength λ and temperature T is given as follows:

$$\ln(I) = A \frac{1}{T} + B, \quad A = -C_2/\lambda, \quad B = \ln\left(\frac{\varepsilon(\lambda)}{\pi} \frac{C_1}{\lambda^5}\right). \quad (6)$$

The logarithmic intensity is linear with respect to the reciprocal of temperature, and coefficients A and B can be obtained by calibration, from which temperature was then derived.

3 Experimental Setup

3.1 Facility Description

Measurements were conducted on a 1-Newton ADN based thruster, as shown in Fig. 3. The experimental ADN thruster was composed of a solenoid valve, an injector, a catalyst bed, a combustion chamber, and a nozzle, while the liquid propellant is composed of 61% ADN, 27% water, and 12% methanol by mass. The catalyst bed was shortened with a length of 14 mm for optimization. A sheathed heater was attached to the outer wall of the catalyst bed for preheating. In the present experiments, steady-state firing was performed at a duration of 10 s and hot firing tests were carried out

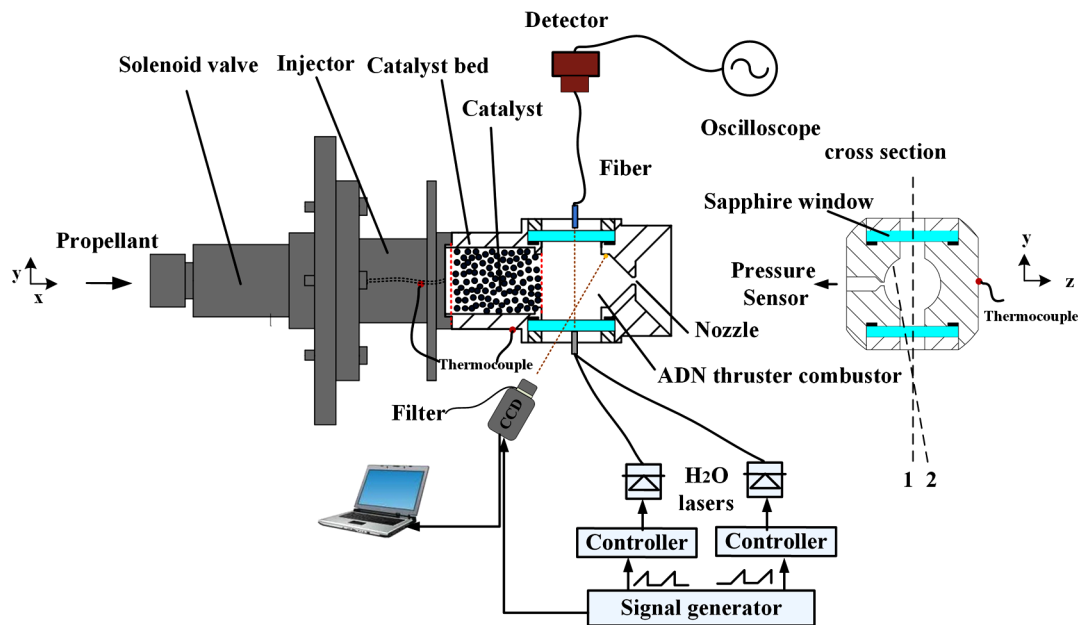


Fig. 2 Layout for temperature measurements in ADN-based thruster.

under various feed pressures of 5 to 12 bar at an ignition temperature of 200°C.

When the thruster operated, the catalyst bed was preheated to the ignition temperature. Upon opening of the solenoid valve, pressurized nitrogen gas forced liquid propellant into the injector, where the propellant was atomized into uniform droplets and subsequently gasified and catalytically decomposed into gaseous intermediates by preheated catalyst particles. Finally, thermal combustion was supported by the intermediates-related reactions in the chamber and combustion exhausts discharged through the nozzle to generate thrust. Laser-based measurements were conducted in the central portion of the combustion chamber, where the chamber dimensions were 10.8 mm in length (x axis) and 8 mm in diameter (y axis). The combustion chamber was manufactured with thicker walls for optical window implementation. Two sapphire windows with 12.7 mm in diameter were installed in the walls of the combustion chamber with 10×3.5 mm² effective light area, as shown in Figs. 1 and 2. All windows were wedged on the outer face to avoid interference from internal etalon-type reflections as laser beams passed through.

3.2 Measurement System

Temperature measurements of combustion gas were performed using two DFB InGaAsP lasers (NEL NLK1B5EAAA) to monitor water vapor absorption at 7185.6 and 7444.3 cm⁻¹, respectively. Two-line thermometry based on the selected absorption lines was developed to be a reliable and secure diagnostic technique and had been applied for varieties of combustion devices with thermometry range of 500 to 2000 K.^{11,19,20} Laser temperature and injection current were modulated by a diode-laser controller (ITC4001, Thorlabs) and wavelength of the laser was tuned using a ramp at a frequency of 1 kHz via a time-division multiplexing strategy. A 2-mm-diameter fiber-coupled collimator was used to ensure the laser beam passing through the optical path closely. Transmitted signals were collected by a multimode fiber

and then detected by an InGaAs detector. The optics and detector were situated close to the window and were purged with nitrogen to remove any interfering absorption by ambient water vapor. A typical measurement of absorption signal at one period was shown in Fig. 3, while Voigt fitting was processed to target transition parameters at 7185.6 and 7444.3 cm⁻¹, respectively. The residual of the fitting exhibits less than 1% error, translating into an error of ~1% in the integrated absorbance and an error of ~2% in the ratio of the integrated absorbance between two transitions. Considering the measurement uncertainty of pressure and optical path-length, measurement error of gas temperature was about 2.7%.¹¹ Temperature nonuniformity along the optical path-length had been carefully evaluated and the cold-flow zone of the boundary layer led to 4.3% variation in temperature measurements, thus we considered gas flow in the cross-section of the chamber was uniform.²¹

For temperature measurements of the inner wall, a monochromatic thermometry system was developed, consisting of a CCD camera mounted with a filter and a PC equipped with a data acquisition system including a frame grabber and system software. Measurements were conducted at position 1 and position 2, respectively, as shown in Fig. 2. In this study, the center wavelength of the filter employed was 780 nm with a bandwidth of 20 nm. The data acquisition system was synchronously triggered with the laser-based sensor by using a signal generator. For monochromatic temperature measurement, experiments were conducted to calibrate the relationship between various temperatures and acquired grayscale of the pixels under the experimental conditions. Figure 4 shows the experimental setup of the monochromatic thermometry calibration. High temperature resistant alloy steel used for the real ADN-based thruster was processed into a thin slice and placed in a tube furnace capable of generating constant temperature environment over the range of 300 to 1400 K. Thermocouples made of platinum-rhodium were installed on the surface of alloy steel and provided accurate temperature sensing. The calibration

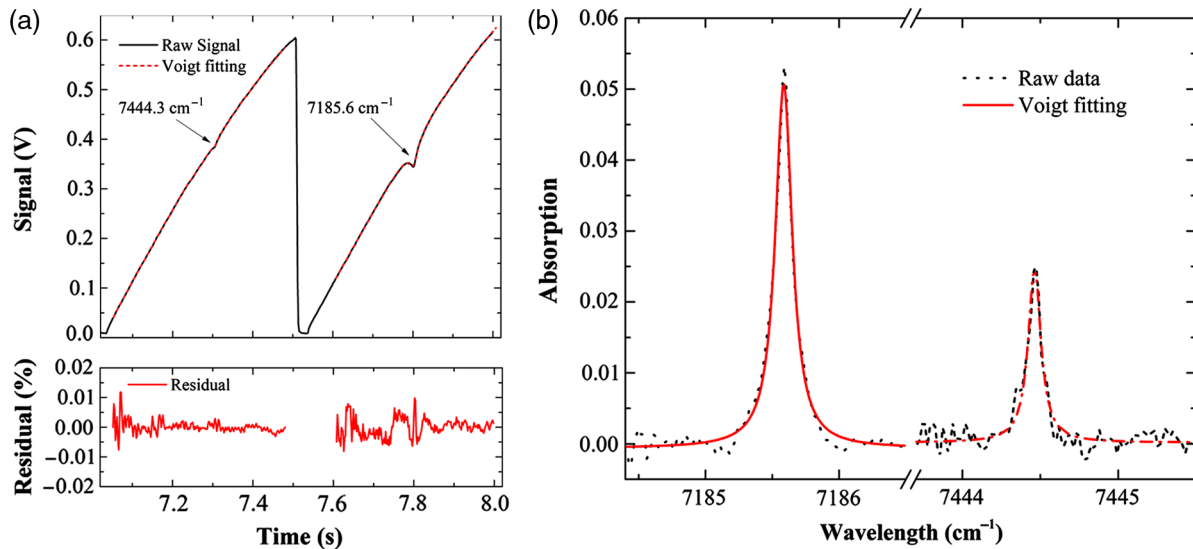


Fig. 3 Measured H₂O absorption and Voigt fitting at one period: (a) raw signal and (b) raw absorption.

procedure was to acquire the frame of radiation of alloy steel and infer pixel grayscale under different temperatures. Figure 5 gives the relationship between various pixel grayscale and temperature. The experimental data agreed with the Wien's approximation, which could be expressed as follows:

$$\ln(N) = -1.57 \times 10^4 \frac{1}{T} + 20.69. \quad (7)$$

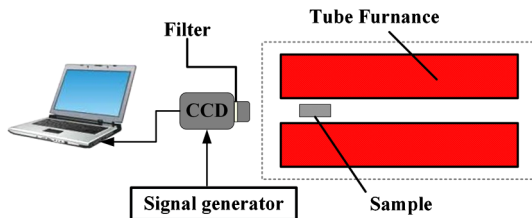


Fig. 4 Layout for monochromatic CCD thermometry calibration.

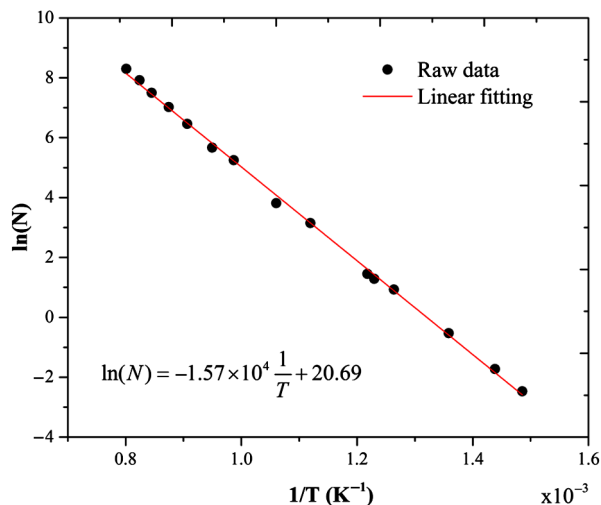


Fig. 5 Relationship between grayscale value and temperature. Experimental data points and approximation based on Wien's law.

Thus, temperature was then derived from the grayscale value of the pixel based on the calibration data.

4 Results and Discussions

Measurements were conducted in an experimental 1N ADN-based thruster under feed pressures of 5 to 12 bar and an ignition temperature of 200°C for 10-s operation. The laser-based sensor and monochromatic thermometry system were simultaneously used to measure temperature of the combustion gas and inner wall in the chamber, respectively. As shown in Fig. 2, three thermocouples made of platinum–rhodium were positioned on the outer wall of downstream of injector, catalyst bed, and combustion chamber, so as to monitor thermal process of the thruster when in operation.

4.1 Temperature Measurement of Combustion Gas Based on Laser-Based Sensor

A steady-state firing test at duration of 10 s was performed under various operation conditions. A feed pressure of 12 bar and an ignition temperature of 200°C corresponded to a

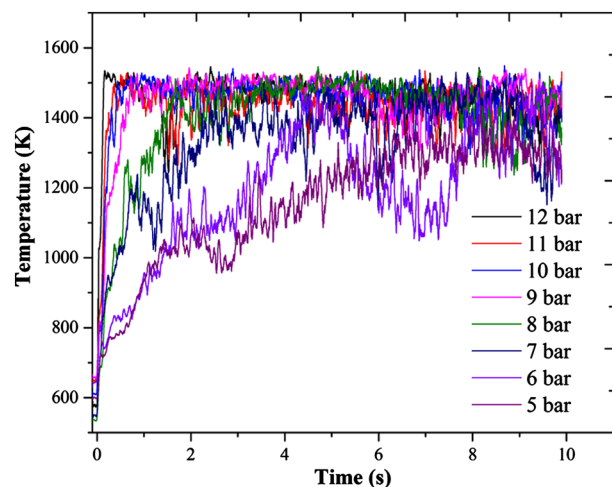


Fig. 6 Measured gas temperature under various feed pressures for 10 s steady-state firing.

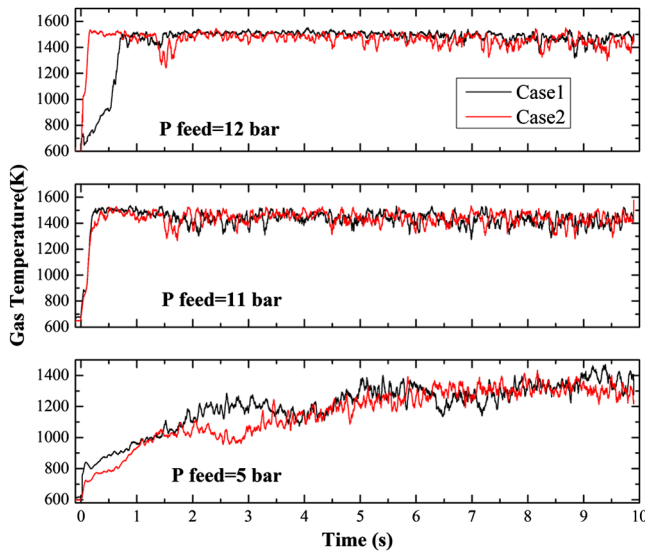


Fig. 7 Comparison of temperature for repeated experiments under different feed pressure.

standard operation condition for the real ADN-based thruster operation. Measured position was installed in the center portion of the combustion chamber along the axis and the thruster operated once the solenoid valve started. Figure 6 shows time history of measured temperature of combustion gas for 10-s operation. For standard operation of the thruster at feed pressure of 12 bar, the temperature quickly raised once the thruster ignited, and then reached equilibrium with a value of nearly 1500 K. Once the feed pressure reduced, equilibrium time of the temperature gradually increased. To be specific, at feed pressures of 8 to 12 bar, the temperature could finally reach equilibrium and the equilibrium value was nearly identical at 1500 K, while experimentally determined temperature for pure ADN combustion at 0.5 MPa was 1350 K²² and the numerical result for

the equilibrium temperature in the combustion chamber when operating an ADN monopropellant thruster was nearly 1600 K.²³ The equilibrium temperature of the wall in the thruster chamber ranged from 1100°C to 1480°C during steady-state firing in the HPGP thruster developed by ECAPS.⁴ At feed pressures of 5 to 7 bar, the gas temperature became unstable, indicating combustion instability in the chamber, which was harmful for thruster operation. Moreover, experiments were conducted repeatedly under different feed pressures to evaluate the stability of the thruster performance.

Figure 7 shows a comparison of gas temperature through two repeated experiments under three feed pressures of 12, 11, and 5, respectively. The measured temperature in two cases showed great consistency under the first two feed pressures and presented difference in temperature measurements under a feed pressure of 5 bar. The measured difference was attributed to combustion instability in the chamber under lower feed pressure operation condition, while reactions of the monopropellant became slower and incomplete. It should be noted that the difference of temperature evolution for the two cases in the early phase of firing at a feed pressure of 12 bar was owing to the reason that case 1 corresponded to the beginning of the whole experiments while the thruster was first ignited.

For laser-based measurement, a preliminary conclusion was presented that there existed a threshold of feed pressure higher than 8 bar for normal operation of the thruster at an ignition temperature of 200°C. An equilibrium temperature of 1500 K was obtained, which was in accordance with previous work, and repeated experiments illustrated excellent thermal stability of the thruster.

4.2 Temperature Measurement of Inner-Wall in the Combustion Chamber

Measurements of the inner-wall temperature were conducted synchronously with gas temperature measurements. A single-monochromatic CCD camera was utilized to grab



Fig. 8 Radiation image of inner wall: downstream of the thruster chamber.

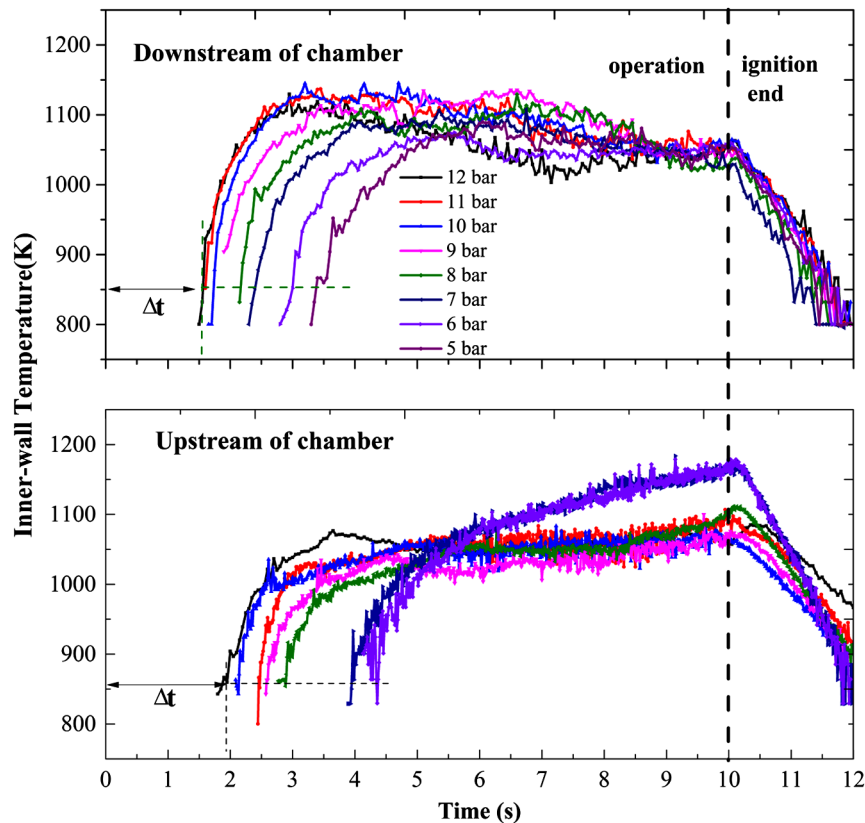


Fig. 9 Measured inner wall temperature of thruster chamber under various feed pressures for 10-s steady-state firing.

the radiation of the inner wall. Figure 8 shows a grabbed image of the inner wall. The measured radiation position was placed in the downstream of the thruster chamber compared with the image of the real thruster. Calibration data between the grayscale of radiation and temperature had been obtained by using the same high temperature resistant alloy steel in a tube furnace. Thus, temperature could be derived from the relationship of the calibration data.

Figure 9 shows upstream and downstream temperatures of the inner wall in the chamber under various feed pressures for 10-s ignition. Once the thruster operated, the temperature of the inner wall increased and reached equilibrium, and the average temperature decreased as the feed pressure reduced, in accordance with evolution of measured gas temperature. The inner-wall temperatures for upstream of the combustion chamber were all quickly reached values of nearly 1000 K as the firing initiated, and then increased as the ignition carried on. Meanwhile, the inner-wall temperatures for downstream of the combustion chamber were all first reached values of nearly 1100 K and decreased as the ignition carried on. Based on the measurements, it could be concluded that heat release zone moved from downstream to upstream in the combustion chamber.

In addition, the author defined the moment that the inner-wall temperature reached a temperature of 850 K as delay time, as shown in Fig. 9. This moment could be instructive for combustion of ADN monopropellant in the chamber. Figure 10 shows the relationship between the delay time and the feed pressure. The delay time of measured inner-wall temperature was monotone decreasing and the growth rate of the delay time gradually reduced to zero as the feed

pressure increased, indicating more complete combustion in the chamber and corresponding to higher performance for the thruster. Over the whole operation feed pressure, the delay time for downstream of the combustion chamber was shorter than the corresponding upstream results, demonstrating faster combustion reactions for the downstream of the combustion chamber.

4.3 Comparison of Measured Gas Temperature and Wall Temperature

Figure 11 shows the measured outer-wall temperature at downstream of the injector, catalyst bed, and combustion

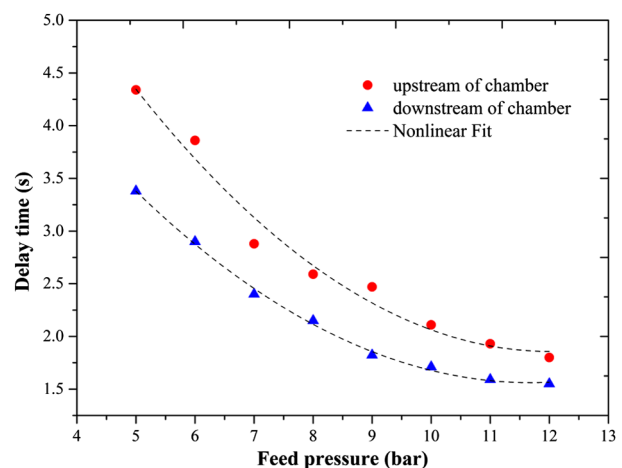


Fig. 10 Delay time (as defined) under various feed pressure.

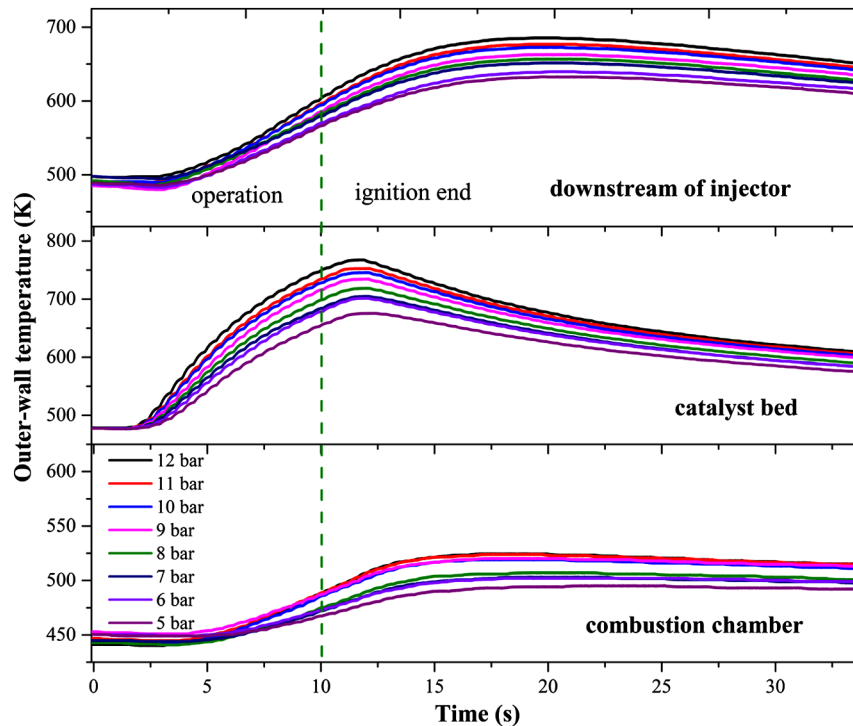


Fig. 11 Measured outer-wall temperature for ADN-based thruster under different feed pressure.

chamber by using thermocouples, respectively. The outer-wall temperatures at the combustion chamber were slowly increased, attributing to a thickened wall of the combustion chamber for window implementation, as shown in Fig. 2, and leading to slower heat transfer from inner wall to outer wall. The outer-wall temperatures at the two other positions increased with time delays and growth rates of the temperature decreased as the feed pressure went down. Over the whole operation feed pressure of 5 to 12 bar, time delays of temperature initiation at downstream of the injector were nearly 3 s, while time delays of temperature initiation at the catalyst bed were shorter with values of nearly 2.5 s, indicating faster heat transfer. Similarly, the maximum temperatures

of the outer wall at the catalyst bed reached faster and were higher than the measurements at downstream of the injector, as shown in Fig. 12. The maximum temperature increased as the feed pressure increased, indicating more complete and quicker reactions for the thruster operation.

5 Conclusions

A combined temperature measurement system by using a laser-based sensor and monochromatic thermometry is performed to monitor temperature of the combustion gas and inner wall in the chamber for a real ADN-based thruster. Experiments are conducted under various feed pressures of 5 to 12 bar for 10-s steady-state firing test. Measured gas temperatures reach equilibrium value of nearly 1500 K under different feed pressures. A preliminary conclusion is presented that a threshold of feed pressure higher than 8 bar is demonstrated to ensure normal and stable operation of the thruster. Results of repeated experiments illustrate thermal stability of the ADN-based thruster. Time-resolved temperature measurements of the inner-wall were in great consistency with measured gas temperature with time delay, in which the time delay reduced as the feed pressure increased. The heat release zone moves upstream in the combustion chamber, which is revealed out of the evolution of the inner-wall temperature in the upstream and downstream of the combustion chamber. This work presents an attempt to quantitatively obtain a thermal process in the thruster so as to analyze its thermal performance. Furthermore, spatial-resolved measurements of temperature along the axial coordinate in the chamber will be extended for future research and provide more useful data to compare with computational fluid dynamics modeling of the whole combustion process of the ADN-based thruster.

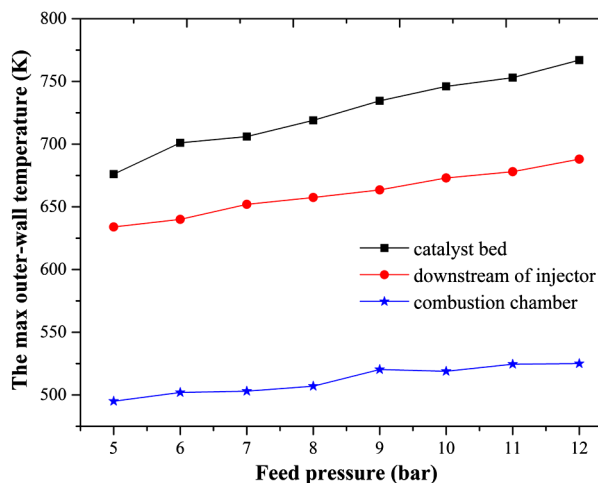


Fig. 12 The max outer-wall temperature under different feed pressure.

Acknowledgments

This work was supported by the National Natural Science Foundation of China (Grant Nos. 11372329 and 90816015).

References

1. A. Larsson and N. Wingborg, "Green propellants based on ammonium dinitramide (ADN)," in *Advances in Spacecraft Technologies*, J. Hall, Ed., pp. 139–156, InTech, Rijeka (2011).
2. K. Anflo et al., "Towards green propulsion for spacecraft with ADN-based monopropellants," in *38th AIAA Joint Propulsion Conf.*, AIAA Paper, Vol. 3847 (2002).
3. M. Lange et al., "Introduction of a high-performance ADN based monopropellant thruster on the Myriade propulsion subsystem technical and operational concept and impacts," in *Proc. 6th Int. Conf. on Recent Advances in Space Technologies (RAST)*, pp. 549–553 (2013).
4. P. Nils, A. Kjell, and S. Oskar, "Spacecraft system level design with regards to incorporation of a new green propulsion system," in *47th AIAA/ASME/SAE/ASEE Joint Propulsion Conf. and Exhibition*, American Institute of Aeronautics and Astronautics (2011).
5. K. Anflo and B. Crowe, "In-space demonstration of an ADN-based propulsion system," in *47th AIAA/ASME/SAE/ASEE Joint Propulsion Conf. and Exhibition*, American Institute of Aeronautics and Astronautics (2011).
6. K. Anflo and R. Mollerberg, "Flight demonstration of new thruster and green propellant technology on the PRISMA satellite," *Acta Astronaut.* **65**, 1238–1249 (2009).
7. P. Childs, J. Greenwood, and C. Long, "Review of temperature measurement," *Rev. Sci. Instrum.* **71**, 2959–2978 (2000).
8. R. K. Hanson, "Applications of quantitative laser sensors to kinetics, propulsion and practical energy systems," *Proc. Combust. Inst.* **33**, 1–40 (2011).
9. X. Zhou et al., "Development of a sensor for temperature and water concentration in combustion gas using a single tunable diode laser," *Meas. Sci. Technol.* **14**, 1459–1468 (2003).
10. H. Li et al., "Near-infrared diode laser absorption sensor for rapid measurements of temperature and water vapor in a shock tube," *Appl. Phys. B* **89**, 407–416 (2007).
11. F. Li et al., "Simultaneous measurements of multiple flow parameters for scramjet characterization using tunable diode-laser sensors," *Appl. Opt.* **50**, 6697–6707 (2011).
12. R. M. Spearrin et al., "Simultaneous sensing of temperature, CO, and CO₂ in a scramjet combustor using quantum cascade laser absorption spectroscopy," *Appl. Phys. B* **117**, 689–698 (2014).
13. F. Meriaudeau, "Real time multispectral high temperature measurement: application to control in the industry," *Image Vis. Comput.* **25**, 1124–1133 (2007).
14. Y. Sun, C. Lou, and H. Zhou, "A simple judgment method of gray property of flames based on spectral analysis and the two-color method for measurements of temperatures and emissivity," *Proc. Combust. Inst.* **33**, 735–741 (2011).
15. M. M. Hossain, G. Lu, and Y. Yan, "Optical fiber imaging based tomographic reconstruction of burner flames," *IEEE Trans. Instrum. Meas.* **61**, 1417–1425 (2012).
16. M. M. Hossain et al., "Three-dimensional reconstruction of flame temperature and emissivity distribution using optical tomographic and two-colour pyrometric techniques," *Meas. Sci. Technol.* **24**, 074010 (2013).
17. M. G. Allen, "Diode laser absorption sensors for gas-dynamic and combustion flows," *Meas. Sci. Technol.* **9**, 545–562 (1998).
18. M. F. Modest, *Radiative Heat Transfer*, Academic Press, San Diego (2013).
19. S. T. Sanders et al., "Diode-laser sensor for monitoring multiple combustion parameters in pulse detonation engines," *Proc. Combust. Inst.* **28**, 587–594 (2000).
20. A. G. Hendricks et al., "The use of tunable diode laser absorption spectroscopy for the measurement of flame dynamics," *Meas. Sci. Technol.* **17**, 139–144 (2006).
21. H. Zeng et al., "Midinfrared absorption measurements of nitrous oxide in ammonium dinitramide monopropellant thruster," *J. Propul. Power* **31**, 1496–1500 (2015).
22. V. P. Sinditskii et al., "Combustion of ammonium dinitramide, part 2: combustion mechanism," *J. Propul. Power* **22**, 777–785 (2006).
23. T. Zhang et al., "Numerical simulation of ammonium dinitramide (ADN)-based non-toxic aerospace propellant decomposition and combustion in a monopropellant thruster," *Energy Convers. Manage.* **87**, 965–974 (2014).

Hui Zeng is an engineer in China Academy of Aerospace Aerodynamics. He is involved in research aimed at optical diagnostic technique for high enthalpy plasma flow. He focuses on flow measurements for aerothermal ground-based testing by using atomic/molecule absorption and emission spectroscopy.

Dongbin Ou is a professor in China Academy of Aerospace Aerodynamics. His research focuses on aerothermal ground-based testing for re-entry vehicle thermal protection system by using variety of arcjet facilities.

Lianzhong Chen is a professor in China Academy of Aerospace Aerodynamics, who leads the Beijing Key Laboratory of Arc Plasma Application Equipment. His research interests include high enthalpy plasma thermal protection system, plasma spheroidization, and plasma processing.

Fei Li is a senior engineer in Key Laboratory of High Temperature Gas Dynamics, Institute of Mechanics, Chinese Academy of Sciences. His research focuses on laser diagnostics by using tunable diode laser absorption spectroscopy (TDLAS), tunable diode laser absorption tomography (TDLAT), and computed tomography of chemiluminescence.

Xilong Yu is a professor in Key Laboratory of High Temperature Gas Dynamics, Institute of Mechanics, Chinese Academy of Sciences. His research focuses on laser diagnostics and application for real combustion environment by using absorption spectroscopy, emission spectroscopy and planar laser-induced fluorescence (PLIF).